Towards the Development of an Online Coverage Path Planner for UUV-based Seafloor Survey using an Interferometric Sonar

Mingxi Zhou*, IEEE Member
Jianguang Shi*‡, IEEE Member
Lin Zhao†
Email:{mzhou, jianguang_shi, linzhao}@uri.edu
*Graduate School of Oceanography, University of Rhode Island, Narragansett, RI, USA
†Ocean Engineering Department, University of Rhode Island, Narragansett, RI, USA
‡Hangzhou Dianzi University, Hangzhou, China

***Abstract*—Seafloor s urvey i s a n i mportant p ractice f or both defense and scientific p urposes. O ften t ime, w e c ould r efer the seafloor s urvey m ission t o a s a c overage p ath p lanning (CPP) problem where the robot has to explore all the points of an area. In this paper, we propose a new online CPP algorithm for a UUV equipped with an interferometric sonar that has inherent problem of nadir gap and changing swath width. The proposed algorithm will account for the above two factors, and schedule new waypoints for the UUV intermittently. The waypoints are determined based on an objective function quantifying the potential measurement accuracy and information gain. We present the algorithm validation in a simulated environment with a 6DOF REMUS AUV model with an actual bathymetric map of Narragansett Bay, Rhode Island. The proposed algorithm is compared to boustrophedon coverage path at different interdistances. In the result, we found advantages of the proposed algorithm in terms of total path length to fully explore a 200 by 500 meters rectangular workspace.**

***Index Terms*—Unmanned Underwater Vehicle, autonomy, coverage path planning, interferometric sonar, seafloor mapping.**

I. Introduction

Seafloor s urvey i s a n i mportant p ractice f or d efense and scientific p urposes, e .g., n aval m ine-countermeasure [1] and seabed habitat and sediment studies [2]. Compared to manned ship surveys, unmanned underwater vehicles provide an alternative approach that is effective in expense, safety and data quality [3].

Often time, we refer the seafloor s urvey t o a s a coverage path planning (CPP) problem where the robot has to explore all the points of an area. CPP is a common problem in robotic research where the robot needs to find t he r oute t o cover every point in an assigned area [4]. Over the years, CPP problem has been studied extensively for a wide variety of applications, e.g., house cleaning, lawn mowing, agriculture monitoring, and underwater explorations. The research focus started with known scenario (known environment and known sensor performance, e.g., in [7]) and partially unknown condition (unknown environment with known sensor performance, e.g., in [8] and [9]). In recenty years, the emphasis started to expand into fully unknown condition (unknown environment and unknown sensor performance, e.g., in [10] to [11]) and multi-robot operations e.g., in [13] to [15]. Detailed surveys about the progress on CPP development are available in [4] to [6]. As mentioned in the literature, the CPP problem for UUVs is still challenging due to the unknown in vehicle performance, e.g., navigation uncertainty, and the performance of perception sensors, e.g., varied sonar swath width [10], [11]. Therefore, an online path-planner like the ones presented in [9] to [11] is needed to fulfill the coverage goal.

In this paper, we will present an online CPP for UUV-based seafloor mapping survey using an interferometric sonar. The CPP will update the UUV's waypoint list intermittently based on the coverage situation that changes during the mission and an inverse-sonar model that provides potential coverage gain and confidence gain on candidate transects. The overall goal is to help the UUV to achieve the desired coverage ratio at reduced total traveling distance compared to conventional boustrophedon path. The main contribution of this paper is summarized as follows,

- The paper presents an CPP algorithm that performs intermittent mission update for the UUV, which lowers the real-time computation requirement.
- The parameters in the CPP algorithms are easy to determine. Most of the parameters could be randomly picked, e.g., the initial waypoint, or automatically calculated, e.g., the expected swath width.
- The transect is not limited in one direction. Instead it could be either zonal or meridional, which allows us to include additional planning factors, e.g., the adverse effects posed by the ocean current.

The remaining content is organized as follows. We will introduce the problem and all the nomenclature in Section

This project is supported by the Department of the Navy, Naval Undersea Warfare Center, Division Keyport, under the Grant Number N00253-19-1-0005.

Authorized licensed use limited to: University of Rhode Island. Downloaded on December 05,2023 at 04:00:54 UTC from IEEE Xplore. Restrictions apply.

978-1-7281-8757-0/20/$31.00 ©2020 IEEE

2. After that, we will present the CPP algorithm in detail in Section 3. In Section 4, we show the preliminary result obtained in a simulation environment where 6 DOF REMUS AUV model and an actual terrain map are used. The results obtained from the proposed CPP are compared with conventional boustrophedon path at different inter-distances. We conclude this paper and discuss our future work in Section 5.

II. Problem Statement

Herein, we define our workspace, M, is gridded into cells. For each cell, $M_{x,y}$ with subscript denoting the cell's location, we define two observation values, the observation state $O_{x,y}$ and the observation confidence $C_{x,y}$. Initially, the observation state and the observation confidence are all set to zero for all cells.

The UUV carries a sonar that scans the workspace during the mission. The sonar swath varies due to the elevation of the seafloor. In each sonar swath, we obtain a group of observed seafloor points relative to the vehicle. Then, we could use the transformation matrix and the vehicle pose information to convert them into an earth-fixed frame. By comparing a point's x and y coordinate, we could identify related cell in the workspace enclosing each point.

If there is a sonar point, $\mathbf{P}_k$, made in a cell, then the cell's observation state $O_{x,y}$ will become 1, meaning observed. Meanwhile, the observation confidence of the cell $C_{x,y}$ is also updated using Equation 1 where $S_{x,y}(k)$ denotes the sensing confidence of the k-th measurement collected inside the cell $M_{x,y}$

$$C_{x,y} = 1 - \prod_{i=1}^{k}(1 - S_{x,y}(\mathbf{P}_k)) \tag{1}$$

$$S_{x,y}(\mathbf{P}_k) = \frac{\frac{R_x^2}{R_z^2} + 0.44\frac{R_x}{R_z} + 0.08}{9.167\frac{R_x^2}{R_z^2} - 29.63\frac{R_x}{R_z} + 28.1416} \tag{2}$$

The sensing confidence curves are different for each sonar. In our case, we used an interferometric sonar. For the interferometric sonar, it has two swaths obtained from the two transducers installed on two sides, as shown in Figure 1. For each sample, we denote the swath on the port and on the starboard side to be L_p and L_s, respectively. The value is determined by the farthest point and the nearest points. These parameters are later used in the coverage path planning software.

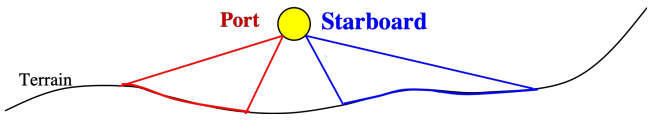

Fig. 1. Two swaths from an interferometric sonar.

For each swath, the confidence curve is determined based on the signal-to-noise ratio presented in [16]. The overall equation is presented in Equation 2 where R_x denotes the cross-track distance between the sonar point and the UUV, and R_z denotes the vertical distance between the UUV and the sonar point. The values are determined by matching the signal-to-noise ratio from [16]. In each swath, we limited the maximum confidence to be 0.9. In Figure 2, we show the confidence curve versus cross-track range and the altitude. The bottom plot depict a cross-section profile of the surface at altitude of 1.5m.

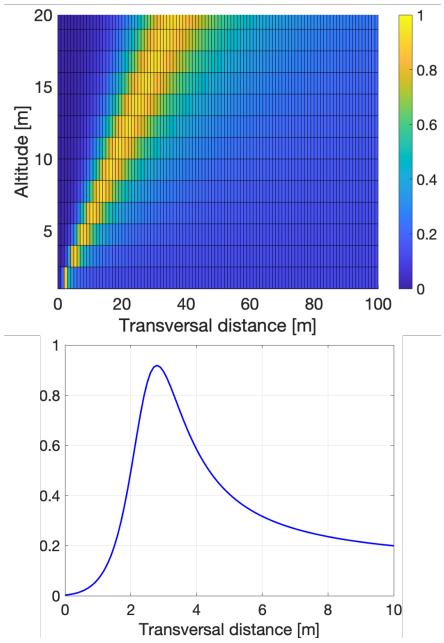

Fig. 2. Top: sensing confidence versus altitude and transversal distance; bottom: sensing confidence over 0 to 10 meters at 1.5 m altitude.

III. CPP Algorithm

The CPP program runs once the UUV has reached the last waypoint on the list. There are three steps in the CPP algorithm. It will first generate the waypoints for all candidate transects. Then, it will quantify the "reward" for each candidate. After the comparison, the CPP will select the path with the highest reward and transmit it to the UUV's operating system.

Figure 3 demonstrates the process of generating candidate waypoints. Overall, there are n possible zonal transects, and m possible meridional transects. The distance between adjacent transects is Δn and Δm. The user could select the adjacent distance freely. A smaller value will result in more candidates and also more computational time. Here, we use the default value, 1 meter, for the transects in both directions. For each candidate transect, the program will shorten it if possible. For example, on the j-th transect in Figure 3, the program predict the possible coverage area based on the minimum swath width observed during the mission, $\min(L_s)$ and $\min(L_p)$. Transect segment in the rectangular region with all the cells observed before will be excluded. As a result, a shorter transect will be obtained with two waypoints located at the end of the reduced transect line.

The next step is to quantify the "reward" of the transect. The CPP program will assume that the UUV will travel to

Authorized licensed use limited to: University of Rhode Island. Downloaded on December 05,2023 at 04:00:54 UTC from IEEE Xplore. Restrictions apply.

the nearest waypoint then follow the transect line moving towards the second waypoint. During this planned travel, the CPP program will predict the possible coverage area, A^j, by assuming the predicted sonar swath width equal to the minimum observed width, $\min(L_s)$ and $\min(L_p)$. The reward consists of two parts, coverage gain (CG) reward and coverage confidence (CC) reward.

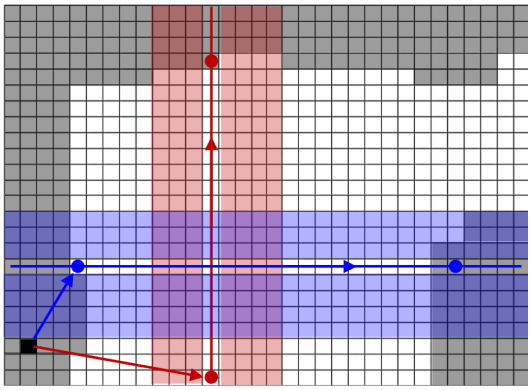

Fig. 3. A sketch demonstrating the waypoint generation process. The gridded map presents the workspace, the black grid indicates the current vehicle position, the red and blue lines presents two examples of candidate transects. The gray area presents the observed cells. The blue and red areas present the predicted sonar coverage, A^j, for corresponding transects. The starboard and port side area may have different widths.The two points on the transects show the final candidate waypoints, and the arrows indicates the vehicle's desired moving trajectory for each transect.

$$CG^j = \frac{\sum O_{x,y}}{D^j} \quad |\forall x, y \in A^j \tag{3}$$

The coverage gain reward is defined to be the total number of possible new observed grids divided by the total travel distance when tracking the candidate waypoints. Equation 3 presents the math expression where the superscript, j, denotes the transect index and D^j is total distance from the UUV's current location to the nearest waypoint plus the transect length. As shown in Equation 4, the confidence gain reward is defined as the total sensing confidence on the unobserved cells that are inside the possible coverage area, A^j.

$$CC^j = \sum O_{x,y} * S_{x,y}(\hat{\mathbf{P}}_k) \quad |\forall x, y \in A^j \tag{4}$$

After the CPP algorithm has estimated the rewards for all the candidate transects, it will rescale CC and CG to 0-100. Then, it will select the most rewarding transect, as shown in Equation 5 where the subscript, s, denotes the scaled values, W_G and W_C are the weights defined by users. We constrain the sum of the weights to be one. The two waypoints associated with the transect $j*$ are the desired waypoints for the UUV to follow.

$$j^* = argmax(W_G * CG_s^j + W_C * CC_s^j) \tag{5}$$

IV. Preliminary Results

The developed CPP algorithm was evaluated in a simulation environment with a 6-DOF REMUS AUV model and a 1-m resolution Digital Terrain Map (DTM) that is interpolated from the 30-m resolution bathymetric map of the Narragansett Bay, Rhode Island. The waypoint tracking of the UUV was realized using the line-of-sight guidance law. The localization error was not introduced because the CPP updates the waypoint intermittently. Therefore, we assume the UUV could come to the surface for GPS fixes or receive geo-referenced location estimates occasionally from acoustic localization instruments, e.g., the LBL, SBL or USBL. Using these information, the UUV could back propagate the trajectory and obtain a relatively accurate geo-location for seafloor surface measurements, hence, minimizing the effects caused by the poor navigation.

In the simulation, we constrain the UUV to move at a constant depth of 10 meters and a constant speed of 1 m/s. The interferometric sonar measurements are simulated using a ray tracing sonar model. In the model, we used the actual sonar parameters, e.g., the field-of-view, the maximum profiling range, and ping rate, which are determined from the sonar specification or found during the initial sonar testing. The swath to altitude ratio was found about 8:1 during our initial sonar testing trials with a boat.

The simulated workspace is 200 m by 500 m with seafloor depth at between 30 to 40 m. In the simulator, we first ran 8 reference missions with boustrophedon patterns at different inter-distances, Δd, from 10 m to 45 m. Then, we ran three missions with the CPP algorithm with reward weights. For these runs, we set the desired coverage ratio to be 99.9%. When the UUV is solely driven by the CG, it will select the transects with the highest newly observed grids regardless of the confidence level of the sample. In contrast, the CC will account for the sensing confidence for the possible newly observed cells, which are derived from a sonar uncertainty model introduced in Section II.

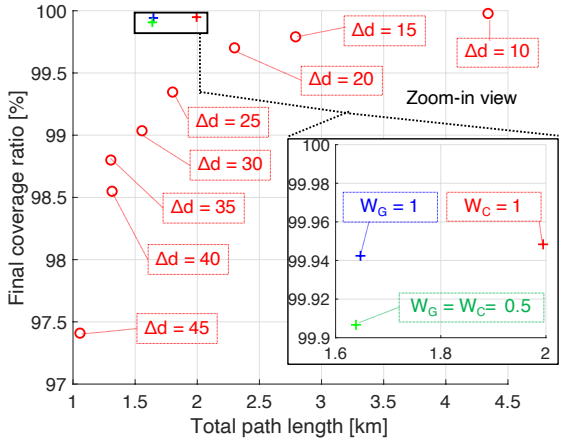

Fig. 4. Comparison of final coverage ratio versus the total traveling distance. Red: offline boustrophedon missions; blue and black: online CPP missions.

Figure 4 shows the final coverage ratio versus the total path length (coverage-distance-ratio) for all simulation runs. The coverage ratio is computed by dividing the number of total observed cells (1m by 1m) by the total number of cells

Authorized licensed use limited to: University of Rhode Island. Downloaded on December 05,2023 at 04:00:54 UTC from IEEE Xplore. Restrictions apply.

in the workspace which is 100,000 in our simulation. The red rounded markers show the results from pre-programmed boustrophedon coverage missions while other markers show that from online CPP algorithms with noted weight settings in the zoom-in view. From the result, we observe that the final coverage ratio in pre-programmed boustrophedon missions increases as the inter-distance between consecutive transects decreases, which follows a logarithm trend. As shown in the figure, three coverage missions with the proposed method all have a final coverage ratio over 99.9%, the desired value. Meanwhile, we found the proposed method over-perform the boustrophedon approach that the total path length of the boustrophedon missions with final coverage ratio exceeding 99.9% are almost two times more.

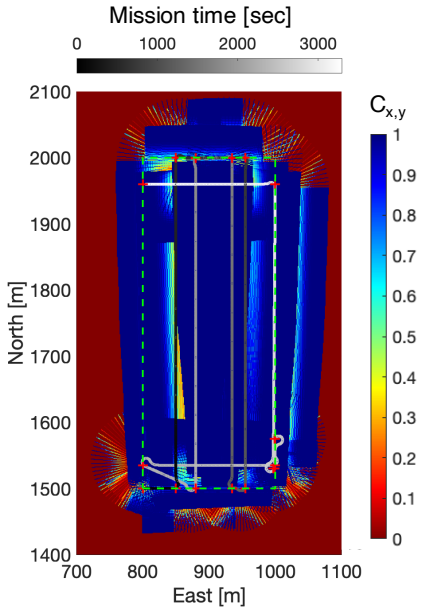

Fig. 5. Final coverage confidence map in the online CPP mission with $W_G = 1$. The red crosses present the waypoint, grey-scale track shows the vehicle trajectory with respect to mission time, the green dashline shows the workspace, and the background color indicates the sensing confidence in grids.

As shown in Figure 4, small difference in coverage-distance-ratio is observed due to the weight changes. Therefore, we further compare the overall sensing confidence in the workspace from all the online CPP missions. For each mission, we computed the sensing confidence in each grid using Equation 1. Figure 5 shows the final sensing confidence in the workspace for the online CPP mission with $W_G = 1$.

In Fig. 6, we show the histogram of the sensing confidence of the workspace from different simulation runs with online CPP. Because good coverage are obtained with the online CPP, the majority of the cells have the sensing confidence over 0.99. Slightly difference in the distributions of the sensing confidence less than 0.99 are found in Fig. 6 In the zoom-in view, the dash-lines show the averaged sensing confidence for all the cells that have sensing confidence less than 0.99 in individual missions. Based on this metric, we found the mission with equal weights for W_C and W_G has the highest mean confidence as the green dash-line is closer to 1. In contrast, when $W_C = 1$, the mission has the lowest mean sensing confidence that the dash-line is under 0.8 and the histogram has a wide and scattered distribution between 1 and 0.2. Both figures, Fig. 4 and 6, indicate that coverage gain, defined in Equation 3, has more influence on the overall coverage mission performance. But including the coverage confidence in addition to the coverage gain, defined in Equation 4, will slightly improve the mission as the green marker has a smaller total distance shown in Fig. 4 and a higher mean sensing confidence shown in Fig. 6. Excluding the coverage gain component in the objective function will increase the overall mission time and lower the sensing confidence as indicated in Fig.4 and 6.

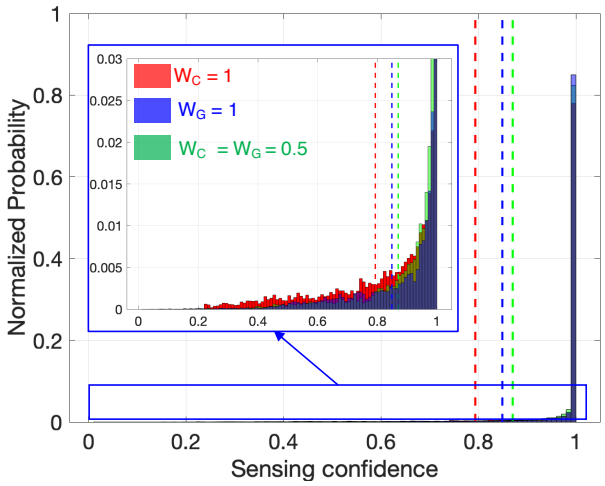

Fig. 6. Histogram of the final mapping confidence of the workspace. The bin size is 0.01. The dash-lines presents the averaged sensing confidence for the grids that have confidence less than 0.99.

V. Conclusion and Future Work

In this paper, we have introduced a new online coverage path planning algorithm using an objective function. The objective function is designed to account for the information of coverage gain and coverage confidence. By selecting the maximum reward transect using the objective function value, the CPP guides the UUV to cover the workspace with a high sensing confidence.

The proposed algorithm has been evaluated in a simulated environment where the modeling modules are implemented using actual specifications for the sonar, UUV, and the seafloor. We compared the results from the proposed CPP method and the conventional boustrophedon planning approach. Compared to the boustrophedon pattern, the UUV could cover 99.9% of the 200m-by-500m workspace using about 50% time with our algorithm. We have also found that the weight assignment in the objective function will affect the overall coverage performance. From the comparison, we found assigning equal weights produced the best results, about 25% faster and 5%

Authorized licensed use limited to: University of Rhode Island. Downloaded on December 05,2023 at 04:00:54 UTC from IEEE Xplore. Restrictions apply.

more confidence than the mission only considered the coverage confidence.

Development is still undergoing. In a real world mission, sonar processing and UUV navigation algorithms are needed. These algorithmic development will be evaluated using the sonar data sets with ground truth localization data and seafloor topography data. We are currently conducting field trials on collecting the data set. The sonar will be integrated onto the UUV during the fall with testing trials in March. Final CPP test will be conducted in spring/summer 2021 in Narragansett Bay, Rhode Island, USA.

REFERENCES

[1] S. Sariel, T. Balch & N. Erdogan, Naval Mine Countermeasure Missions. IEEE Robotics & Automation Magazine, (March), 45–52, 2008.

[2] N. Tolimieri, M. Clarke, H. Singh, & C. Goldfinger, Evaluating the SeaBED AUV for Monitoring Groundfish in Untrawlable Habitat, Marine Habitat Mapping Technology for Alaska, 129–142, 2008.

[3] D. W. Caress, H. Thomas, W. J. Kirkwood, R. McEwen, R. Henthorn, D. A. Clague, C. K. Paull, J. Paduan & K. L. Maier, High-resolution multibeam, sidescan, and subbottom surveys using the MBARI AUV D. Allan B, Marine habitat mapping technology for Alaska, 47–69, 2008.

[4] T. Cabreira, L. Brisolara & P. R. Ferreira, Survey on Coverage Path Planning with Unmanned Aerial Vehicles, Drones, vol. 3, no. 1, 2019.

[5] H. Choset, Coverage for robotics – A survey of recent results, Annals of Mathematics and Artificial Intelligence, vol. 31, pp.113-126, 2001.

[6] E. Galceran & M. Carreras, A survey on coverage path planning for robotics, Robotics and Autonomous Systems, vol. 61, no. 12, pp. 1258–1276, 2013.

[7] H. Choset, & P. Pignon, Coverage Path Planning: The Boustrophedon Cellular Decomposition. In: Zelinsky A. (eds) Field and Service Robotics. Springer, London, 1998

[8] B. Englot & F. S. Hover, Sampling-based coverage path planning for inspection of complex structures, The 22nd International Conference on Automated Planning and Scheduling, 29–37, 2014.

[9] E. Galceran & M. Carreras, Efficient seabed coverage path planning for ASVs and AUVs, IEEE International Conference on Intelligent Robots and Systems, 88–93, 2012.

[10] L. Paull, S. Saeedi, M. Seto & H. Li, Sensor-Driven Online Coverage Planning for Autonomous Underwater Vehicles, IEEE/ASME Transactions on Mechatronics, vol. 18, no. 6, pp. 1827-1838, 2013.

[11] E. Galceran, R. Campos, D. Ribas, M. Carreras & P. Ridao, Coverage Path Planning with Real-time Replanning and Surface Reconstruction for Inspection of Three-dimensional Underwater Structures using Autonomous Underwater Vehicles, Journal of Field Robotics, vol.32, no.7, pp.952–983, 2015.

[12] E. Galceran & M. Carreras, Planning coverage paths on bathymetric maps for in-detail inspection of the ocean floor, IEEE International Conference on Robotics and Automation, 4159–4164, 2013.

[13] N. Karapetyan, J. Moulton, J. S. Lewis, A. Q. Li, J. M. Okane & I. Rekleitis, Multi-robot Dubins Coverage with Autonomous Surface Vehicles, IEEE International Conference on Robotics and Automation, 2373–2379, 2018.

[14] I. Rekleitis, V. Lee-shue, A. P. New & H. Choset, Limited Communication, Multi-Robot Team Based Coverage, IEEE International Conference on Robotics and Automation, 3462–3468, 2004.

[15] I. Rekleitis, A. Peng, N. Edward & H. Choset, Efficient Boustrophedon Multi-Robot Coverage : an algorithmic approach, Annals of Mathematics and Artificial Intelligence, vol.2008, no.52, pp.109–142.

[16] J. Singh, C. Ioana, M. Geen, J. Mars, Interferometric Measurements with Wide-band Signal Processing Techniques, OCEANS'19 MTS/IEEE, Jun 2019, MARSEILLE, France.

Authorized licensed use limited to: University of Rhode Island. Downloaded on December 05,2023 at 04:00:54 UTC from IEEE Xplore. Restrictions apply.